

Predicting the response of polyurea coated high hard steel plates to ballistic impact by fragment simulating projectiles

M. Irshidat ⁽¹⁾, A. Al-Ostaz ⁽²⁾, and A.H.-D. Cheng ⁽³⁾

Abstract

The response of polyurea coated High Hard Steel (HHS) plates to ballistic impact by Fragment Simulating Projectiles (FSP) is investigated using nonlinear dynamic computational analysis. A series of simulations was performed using hydrocode AUTODYN to predict ballistic limit (V_{50}) of target plates. Comparing the computational results with those from published experiments show that the numerical models have the ability to predict with reasonable confidence the V_{50} of reference uncoated HHS plates and polyurea coated HHS plates. The numerical results show that mode of failures of reference uncoated HHS plate to the fragment simulating projectile can be divided into four categories: dishing mode at low-impact velocity, shear plug at intermediate velocities, full penetration at higher velocities, and complete fragmentation of penetrated area. It is found that whereas coating the impacted face of the HHS plates with polyurea does not improve their fracture patterns, it leads to an increase in their ballistic limit. Therefore, the polyurea may serve as a protective layer that could delay the fracture of the steel plate and thus increases the energy absorption.

Keywords: Polyurea; Ballistic impact; Fragment simulating projectile; AUTODYN.

⁽¹⁾ Nano Infrastructure Research Group-Department of Civil Engineering, University of Mississippi, Oxford, Mississippi, 38677-1848, USA

⁽²⁾ Nano Infrastructure Research Group-Department of Civil Engineering, University of Mississippi, Oxford, Mississippi, 38677-1848, USA

⁽³⁾ Nano Infrastructure Research Group-Department of Civil Engineering, University of Mississippi, Oxford, Mississippi, 38677-1848, USA

1 Introduction

Elastomers (e.g. polyurea) are highly viscoelastic and thus their mechanical properties are strongly rate-dependent (Ronald et al [1]). The viscoelastic response of polyurea underlies many applications involving high strain-rates associated with ballistic impact. The attraction of polyurea for ballistic resistance applications is that it is formed *in situ* by the rapid reaction of isocyanates with polyamines. The physics of ballistic penetration of hard targets has been the focus of many investigations [2, 3]. However, the origin of the ballistic mitigation using rubber coatings is not fully understood because of the complex mechanisms involved [4-6].

A review of the literature revealed the existence of many material models developed for polyurea. Amirkhizi et al. [7] reported an experimentally-based pressure-sensitive linear viscoelastic constitutive model which utilizes the classical Williams–Landel–Ferry (WLF) time–temperature transformation/superposition. Elsayed et al. [8, 9] developed a model to describe the behavior of polyurea as a network of parallel hyperelastic and elastic viscoplastic branches. The hyperelastic branches are modeled using a higher order Ogden strain energy density function while the elastic viscoplastic branches are modeled as a collection of springs and dashpots of different stiffness and relaxation times. Li and Lua [10] represented a simple superposition of a hyperelastic material model and a nonlinear viscoelastic material model. The hyperelastic part of the material model was represented using the Ogden strain energy density function and is parameterized by using the quasi-static loading stress–strain data. The viscoelastic part of the model, on the other hand, is based on a deformation-history functional and is parameterized by using shear-modulus relaxation test data.

Several researchers studied the feasibility of using polyurea to improve the ballistic resistance of steel plates. Roland et al. [11] showed that polyurea, when coat the front face of the steel plates, provided a significant enhancement in the ballistic-penetration resistance of these plates with respect to the impact by fragment simulating projectiles (FSP). Roland and coworkers [12] concluded that the most logical choice of mechanism that could be responsible for the observed improvement in ballistic impact resistance of the polyurea-coated steel plates is a phase transition of the polyurea from the rubbery to the glassy state. Grujicic et al. [13] provided computational support for the ballistic resistance improvement mechanism based on the deformation-induced glass transition as proposed in [11, 12]. Xue et al. [14] studied experimentally and numerically the impact resistance of a blank DH-36 steel plates, steel plates with polyurea backing, and sandwich plates subjected to both pointed and flat projectiles. They found that the polyurea coating provided additional resistance in terms of energy absorption through two mechanisms: (1) the increase in the energy dissipated by the steel plate and (2) the increased energy stored in the polyurea itself. In the contrast with other researchers, Amini et al. [15] found that the polyurea layer can have a significant effect on the response of the steel plate under dynamic impulsive loading both in terms of failure mitigation and energy absorption, only if it is deposited on the back face of the plate. Remarkably, when polyurea is placed on the front face (i.e., the blast-receiving face) of the plate, it may actually enhance the destructive effect of the blast, promoting (rather than mitigating) the failure of the steel plate.

In the present work, a nonlinear dynamic analysis of the impact and penetration of High Hard Steel (HHS) plates with and without polyurea coatings is carried out in order to predict its response to ballistic impact by fragment simulating projectiles. The simulation results are compared with the corresponding experiments carried out by Roland and coworkers [12]. The main features that are compared between the numerical and experimental results are the

deformations and damage status of the steel plate and the polyurea coating, and the residual velocities of the projectile. Particular emphasis has been placed on the energy absorption capacity of the polyurea layer and the steel plate.

The organization of the paper is as follows. A detailed description of the material models assigned to the polyurea coating and the steel test plate is provided in Section 2. A brief overview of the problem studied in the present work is given in Section 3.1. Details of the numerical model used to analyze the impact of the target plate by the fragment simulating projectile are presented in Section 3.2. The results obtained in the present work are presented and discussed in Section 4. The main conclusions resulting from the present work are summarized in Section 5.

2 Material modeling

In a hydrocode simulation, the response of a continuum subjected to dynamic loading is governed by the conservation of mass, momentum and energy, the equation of state (EOS), and the constitutive relation of the continuum. These equations arise from the fact that the total stress tensor can be decomposed into a sum of a hydrostatic stress tensor and a deviatoric stress tensor. An equation of state then is used to define the corresponding relationship between pressure, specific volume, and internal energy density, while a strength relation is used to define the appropriate equivalent plastic-strain, equivalent plastic-strain rate, and temperature dependencies of the yield surface. In addition, a material model generally includes a failure criterion. A detailed account of the constitutive models for the materials used in the present work (hard steel and polyurea) is given in this section. The values of all the material parameters defined here are available in the AUTODYN materials library [16].

2.1 Hard steel (4340 Steel)

Equation of state

For 4340 steel material, the linear equation of state is used which assumes a Hooke's law type relationship between the pressure (P) and the volume change $\mu = \left(\frac{\rho}{\rho_0} - 1\right)$ as:

$$P = K\mu \quad (1)$$

where K is the bulk modulus of the material.

Strength model

The most commonly used strength model for steel material subjected to high strain-rates, large deformation, and high temperature is the Johnson-Cook model. The yield stress σ at non-zero strain rate, depends on the strain hardening, strain rate hardening, and temperature softening, such that

$$\sigma = [A + B\varepsilon_{pl}^n][1 + C\ln\dot{\varepsilon}_{pl}][1 - T_{H0}^m] \quad (2)$$

where ε_{pl} is the equivalent plastic strain, $\dot{\varepsilon}_{pl}$ the equivalent plastic strain rate, A , B , and C are material parameters (A initial yield stress, B hardening constant, and C strain rate constant), n and m are respectively the hardening exponent and thermal softening exponent, and $T_{H0} = (T - T_{room}) / (T_{melt} - T_{room})$ nondimensional normalized (homologous) temperature (room temperature (T_{room}) while T_{melt} is the melting temperature). All temperatures are given in Kelvin.

Failure model

For 4340 steel that fails in a ductile mode, the failure condition is defined mostly using the Johnson-Cook failure model [17]. The progress of failure according to the Johnson-Cook failure model is based on the damage parameter D . Failure occurs when the value of D exceeds 1.

$$D = \sum \frac{\Delta\varepsilon}{\varepsilon_f} \quad (3)$$

where $\Delta\varepsilon$ is the increment in effective plastic strain and ε_f is the strain at failure, which is a function of the mean stress, the effective stress, the strain rate, and the homologous temperature, given by:

$$\varepsilon_f = [D_3 + D_4 \exp(D_5 \sigma^*)][1 + D_6 \ln \dot{\varepsilon}_{pl}][1 + D_7 T_{H0}] \quad (4)$$

where σ^* is mean stress normalized by the effective stress. The parameters D_3 , D_4 , D_5 , D_6 and D_7 are all material specific constants.

2.2 Polyurea

Equation of State

For polyurea, the linear equation of state (equation 1) is used.

Strength Model

The polyurea stress-strain relationship is described by the following relation:

$$\sigma = (A\varepsilon^6 + B\varepsilon^5 + C\varepsilon^4 + D\varepsilon^3 + E\varepsilon^2 + F\varepsilon + G) \times (1 + H * \ln \dot{\varepsilon}) \quad (5)$$

The quasi-static behavior of the polyurea fits a six-order polynomial, while the strain-rate dependency is covered in the second term (the logarithmic term). The model parameters are summarized in Table 1. Ronald et al. [1] tested polyurea in a simple tension test at high strain-rates. Fig.1 shows the stress-strain relationship for the polyurea at different strain rates.

Table 1 Material parameters for polyurea

A	B	C	D	E	F	G	H
69.5	-262.2	364.6	-197.3	17.9	42.7	0.6	0.1

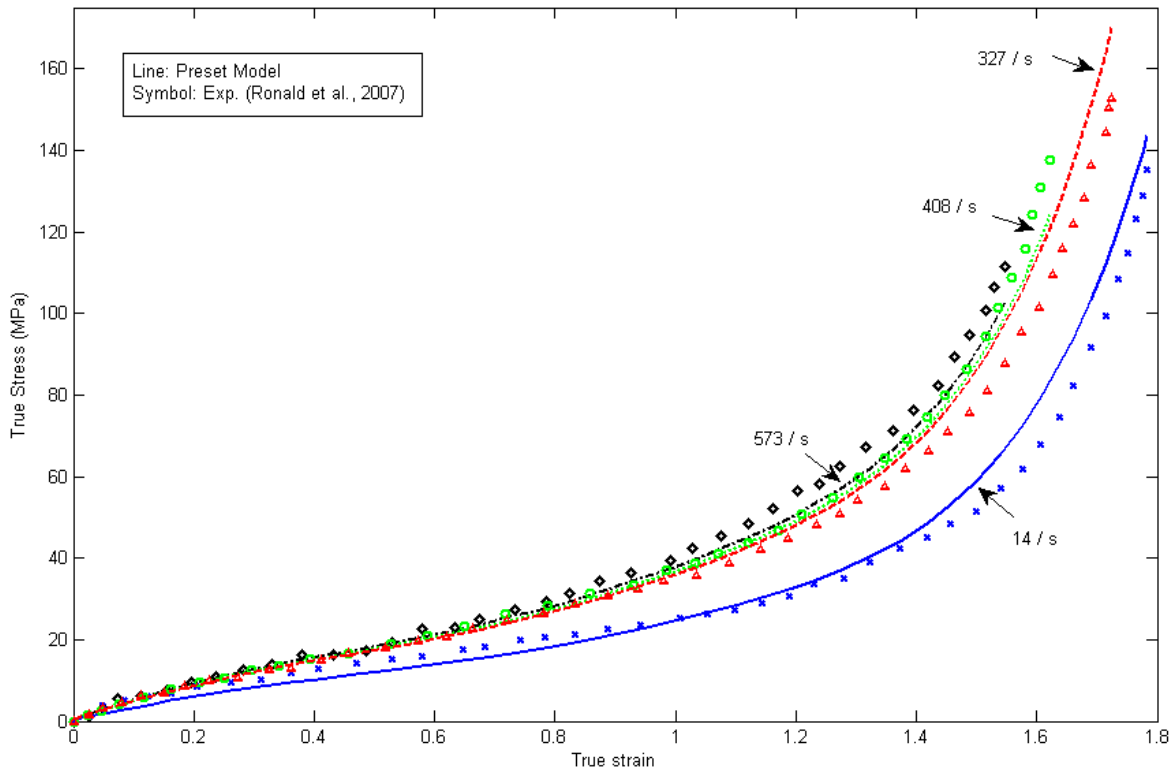


Fig. 1 The stress-strain relationship for the polyurea at different strain rates. Experimental results are from Ronald et al. [1]

3 Computational procedure

Computer programs that are capable of computing strains, stresses, velocities, and propagation of shock waves as a function of time and position are known as hydrocodes [16, 18]. Hydrocode software is suited for modeling explosion, blast, and impact problems. In the present work, the hydrocode simulations are performed using AUTODYN [16], a fully integrated and interactive code specifically designed for nonlinear dynamic problems. One unique feature of AUTODYN is that it allows different parts of a problem to be modeled with applicable and available numerical formulations. This allows users to choose a solution technique driven by the physical nature of the problem and to couple different solution techniques for a given problem. The Lagrange technique is typically used for solid continuum and structures, and the Euler technique is commonly used for modeling gases, liquids or solids subject to large deformations. Solid continuum and structures are also analyzed using the SPH (Smooth Particle Hydrodynamics) a technique that does not suffer from a grid tangling problem (typically encountered in Lagrange processor) and does not require the use of an unphysical erosion algorithm (removal of highly distorted grids to help the numerical procedure). In the present work, both Lagrange and SPH techniques are employed. They are each assigned to the target plate and are compared based on their ability to predict the ballistic limit V_{50} .

3.1 Problem definition

In the present work, a nonlinear dynamic analysis of the impact and penetration of High Hard Steel (HHS) plates with and without polyurea coatings is carried out in order to predict their response to ballistic impact by fragment simulating projectiles. Since the simulation results are compared with the corresponding experiments carried out by Roland and coworkers [11], the hydrocode model was constructed to replicate the experimental set-up used in [11].

The impact configurations of the projectile on two types of target plates are shown in Fig. 2. The first type of target plate is a 12.7mm-thick blank HHS plate (Fig. 2 (a)). The second type of target plate is the same steel plate, but coated by a 12.7mm-thick polyurea layer on the front side of the plate (Fig. 2(b)).

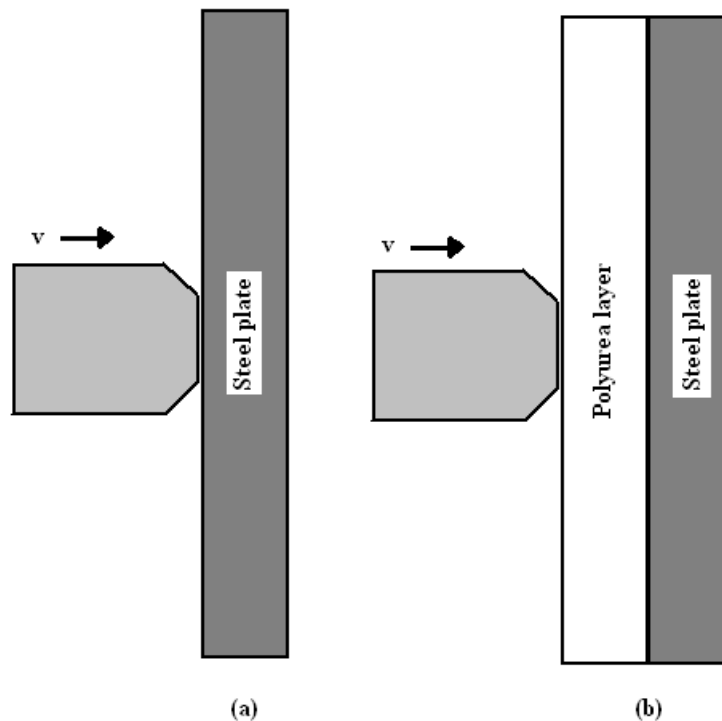


Fig. 2 Sketch of the impact scenarios of the fragment simulating projectile onto (a) Blank HHS steel plate (b) Polyurea coated HHS plate

3.2 Hydrocode model and computational analysis

A Fragment simulating projectile made of 4340 steel is modeled using the Lagrange numerical formulation for all simulations. The projectile domains were discrete using a mesh consisting of 180 rectangular cells. Fig. 3 presents the geometry and the mesh of the projectile. Due to the axial-symmetry nature of the problem, all simulations are carried out using a two-dimensional axisymmetric model.

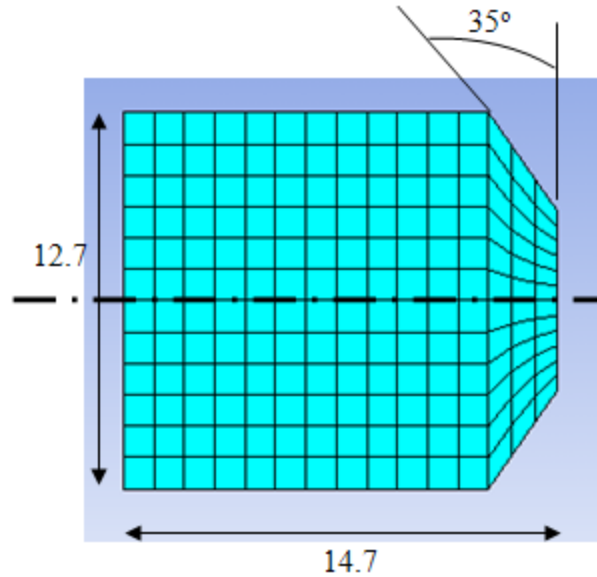


Fig. 3 The mesh of the fragment simulating projectile; all dimensions are in mm

In order to predict the ballistic limit (V_{50}) of the target plates, four separate sets of simulations were carried out. In the first two sets, the plate was modeled using the Lagrange technique while in the other two sets the SPH technique was employed. At the beginning of each simulation, a constant initial velocity is assigned to the projectile in the normal direction of the plate.

3.2.1 Lagrange solution technique

The target plate was modeled using a Lagrangian mesh. For the case of blank steel plate, 1440 rectangular cells were used to represent the plate. For the polyurea coated steel plate, another 1440 cells were added to model the polyurea coating layer. To improve the accuracy of the analysis, smaller cells were used in the region of the projectile. Fig. 4 shows the impact region of the target plate.

Since the target plates will experience severe deformation during the penetration, calculations using the Lagrange solution technique will result in excessive cell distortion and tangling. To prevent the calculation from terminating prematurely due to cell distortion and tangling, an erosion logic based on an incremental geometric strain is assigned to the plate. The erosion logic, which is not a representation of the physical process, automatically removes the distorted cells when the incremental geometric strain of these cells exceeds a predefined setting. To ensure that the cells are not severely eroded and the erosion does not affect the calculation, the erosion is set to 300%.

3.2.2 SPH solution technique

In the case of the SPH technique, the target plate was represented by 1 mm-particles resulting in 3048 interpolation particles to model the blanked steel plate and another 3048 particles to model the polyurea coating layer. Unlike the Lagrangian solution technique, the SPH particles do not suffer from cell distortion and tangling when solving large deformation problems. Fig. 5

shows impact regions of the target plate model using SPH technique.

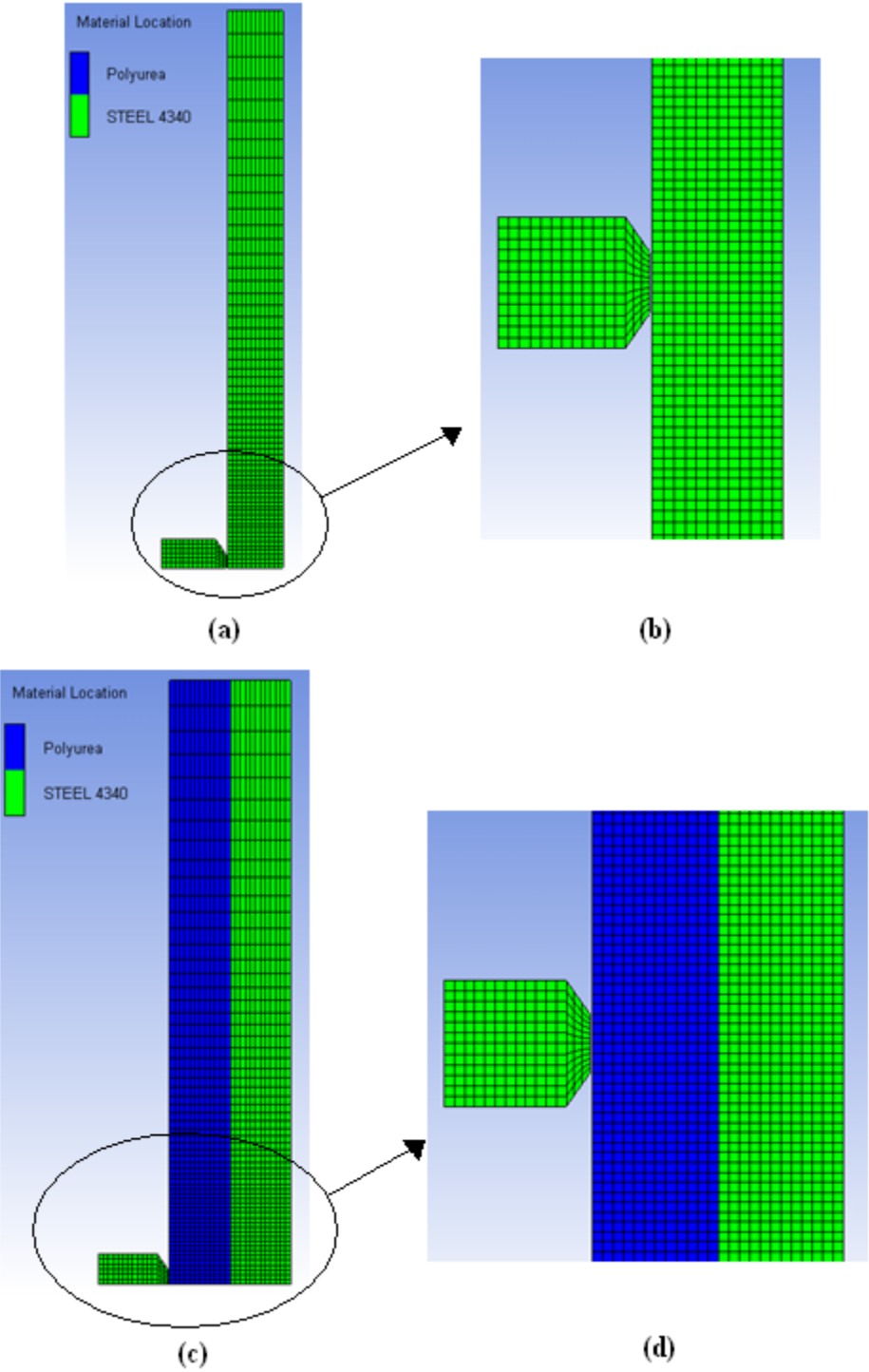


Fig. 4 Mesh size and impact regions of the target plate for Lagrange solution technique, (a) and (b) for blank steel plate while (c) and (d) for polyurea coated steel plate.

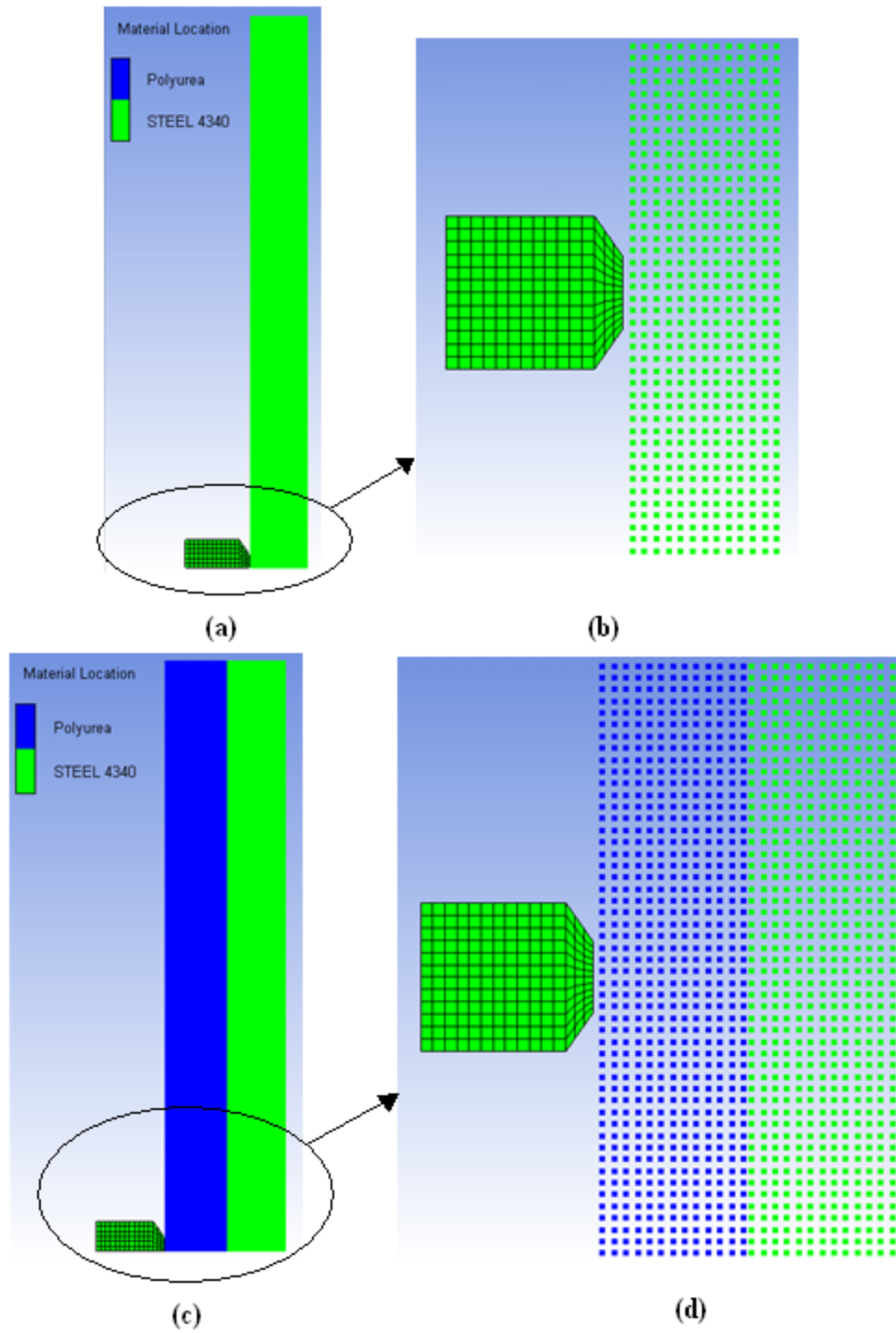


Fig. 5 Particle size and impact regions of the target plate for SPH solution technique, (a) and (b) for blank steel plate while (c) and (d) for polyurea coated steel plate.

4 Results and discussions

4.1 Effect of the solution technique on predicting the ballistic limit (V_{50})

As mentioned earlier, both Lagrange and SPH techniques are employed in this research to predict the ballistic limit V_{50} of blank HHS plates and polyurea coated HHS plates. The size of the mesh in the case of the Lagrange processor and the size of the particles in the case of the SPH processor were selected in such a way that their further refinement does not measurably affect the computed results. Table 2 compares the ballistic limit of the blank HHS plate and polyurea coated HHS plate predicted numerically with the data obtained from experiments by Ronald et al. [11].

Table 2 Ballistic limit (m/s) of blank HHS plate and polyurea coated HHS plate predicted numerically and experimentally, experimental results from Ronald et al. 2007 [1]

Solver	SPH	Lagrangian	Experimental
Blank HHS plate	1300	1450	1184
Polyurea coated HHS plate	1500	1750	1483

Comparing the computational results with those from the experiments shows that simulations using SPH technique have the ability to predict the V_{50} of the target plates more accurate than Lagrange technique. We may attribute this to the erosion strain. When an element erodes, all of the stresses in that element are instantaneously set to zero. In the case of using SPH technique, there is no erosion strain to prevent mesh tangling in the target. Thus, their results provide a much better agreement with the experimental test results. Since there are no guidelines for the selection for a magnitude of the erosion strain, the SPH processor appears to be a preferred computational approach for analysis of the ballistic performance of the polyurea coated HHS plates. All the results presented in the following sections were obtained using SPH technique.

4.2 Ballistic performance of blank HHS

First, we study the penetration of the blank HHS plate by the fragment simulating projectile at various velocities. A series of simulations of this projectile striking blank plates were run with impact velocities ranging from 800 to 2500 m/s. Different deformation and fracture patterns were observed in the blank plates (Figs. 6 and 7).

The response of the blank HHS plate to the fragment simulating projectile can be divided into four categories. (a) At impact velocities below V_{50} , dishing mode was observed. The kinetic energy of the projectile is dissipated by the plastic deformation of the plate. (b) At impact velocities just a little above V_{50} , a shear plug is broken off the steel plate right underneath the impacted area of the projectile. However, the projectile was stopped. (c) At higher velocities, the projectile makes its way through the entire thickness of the steel plate. (d) At even higher impact velocities, complete fragmentation of the penetrated area into small pieces was observed.

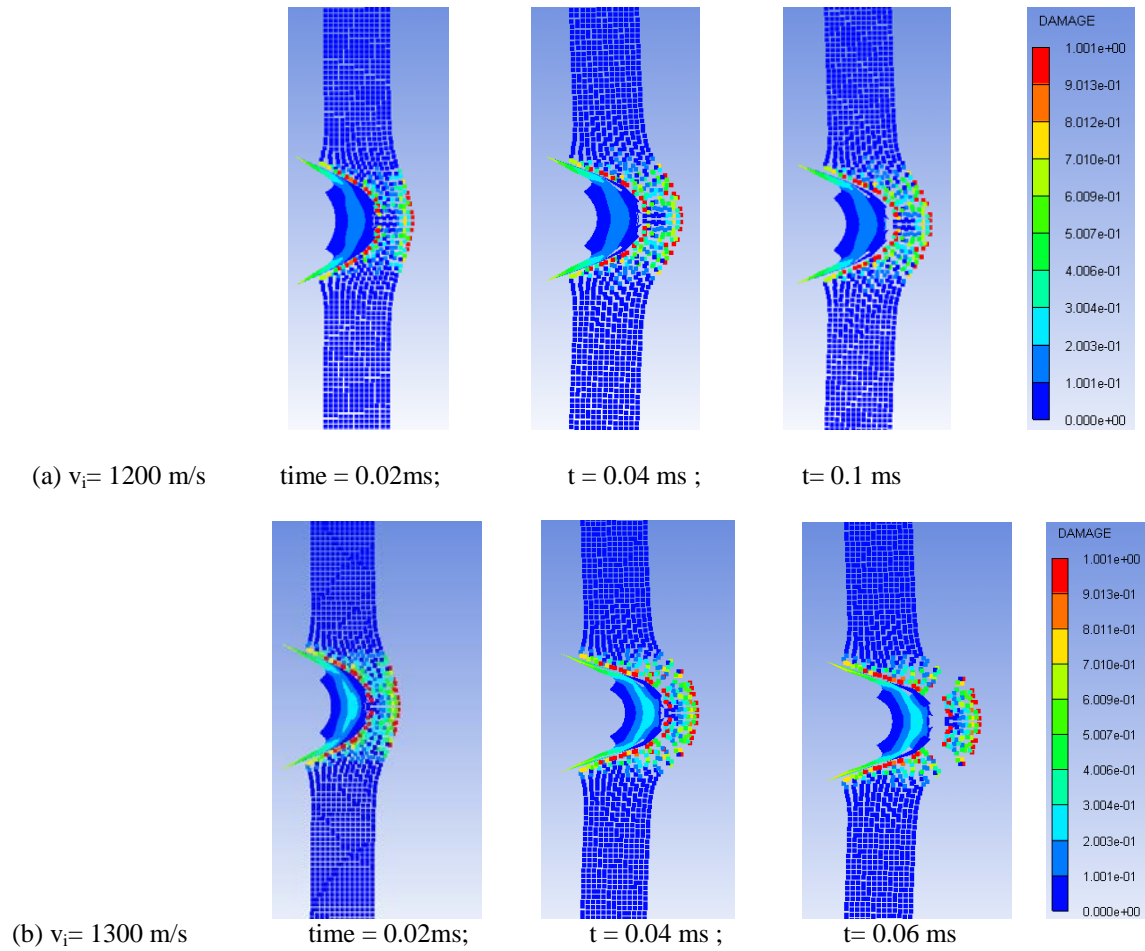
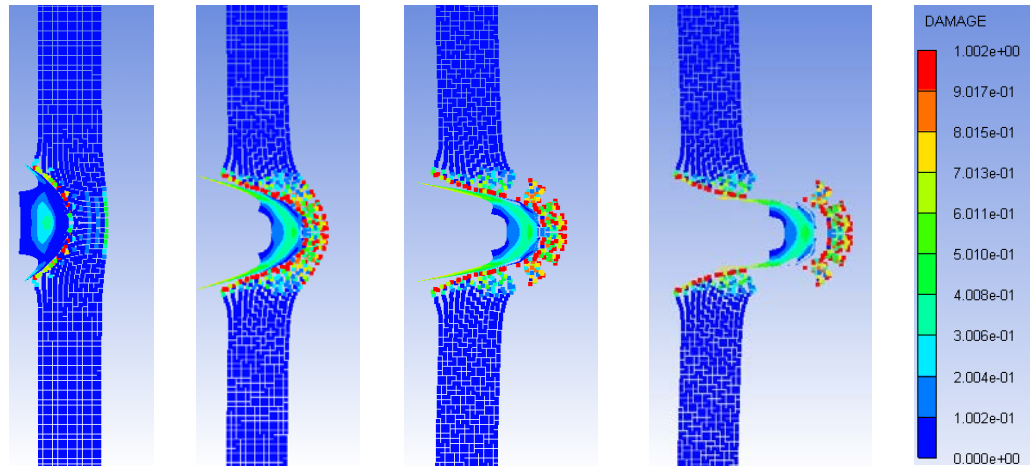
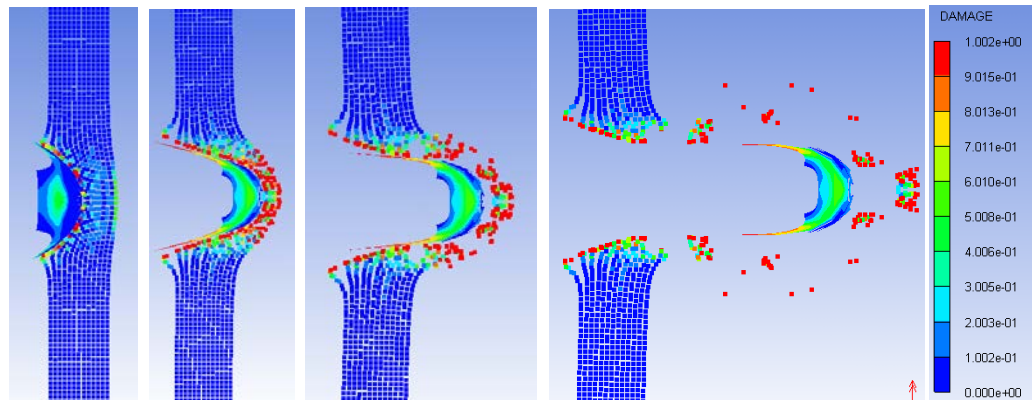


Fig. 6 Deformation and damage status vary at different impact velocities for blank HHS plate impacted by fragment simulating projectiles at velocities (a) 1200 m/s (b) 1300 m/s

Fig. 8 illustrates the nonlinear relationship observed between the velocity of the fragment simulating projectile at impact and its residual velocity after penetration of the blank HHS plate. Both impact and residual velocities are normalized by ballistic limit (V_{50}).



(a) $v_i = 1500$ m/s time = 0.008ms; $t = 0.024$ ms ; $t = 0.038$ ms ; $t = 0.067$ ms



(b) $v_i = 1700$ m/s time = 0.008ms; $t = 0.024$ ms ; $t = 0.038$ ms ; $t = 0.082$ ms

Fig. 7 Deformation and damage status vary at different impact velocities for blank HHS plate impacted by fragment simulating projectiles at velocities above 1500 m/s

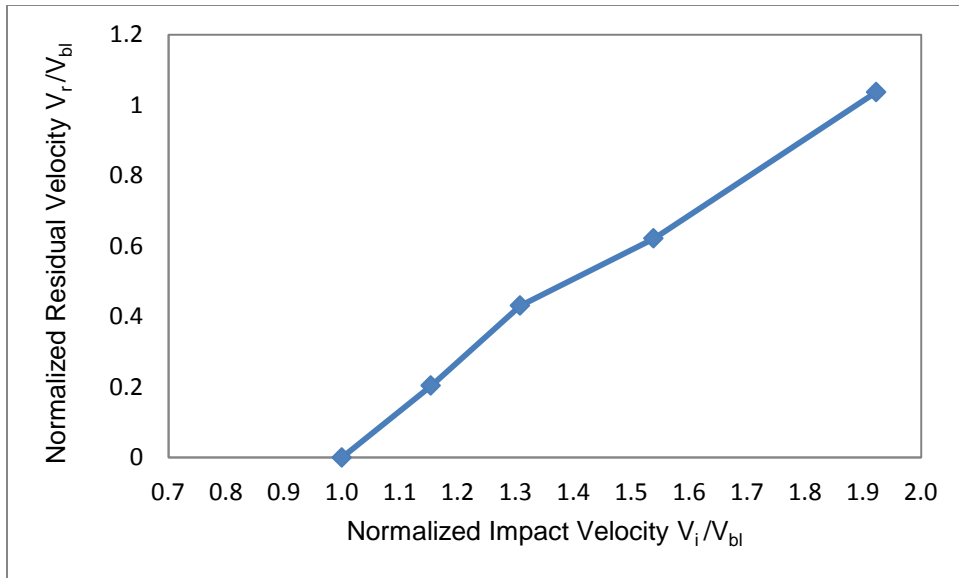


Fig. 8 The residual velocities vs. the impact velocities of the projectile when impacting on blank steel plate

The energy absorption of the blank steel plate at the range of the impact velocities by a fragment simulation projectile is plotted in Figs. 9 and 10. The energy dissipated by the target plate (E_{plate}) is normalized by the initial kinetic energy of the projectile at the ballistic limit $E_{bl} = 1/2 m_{proj} v_{bl}^2$.

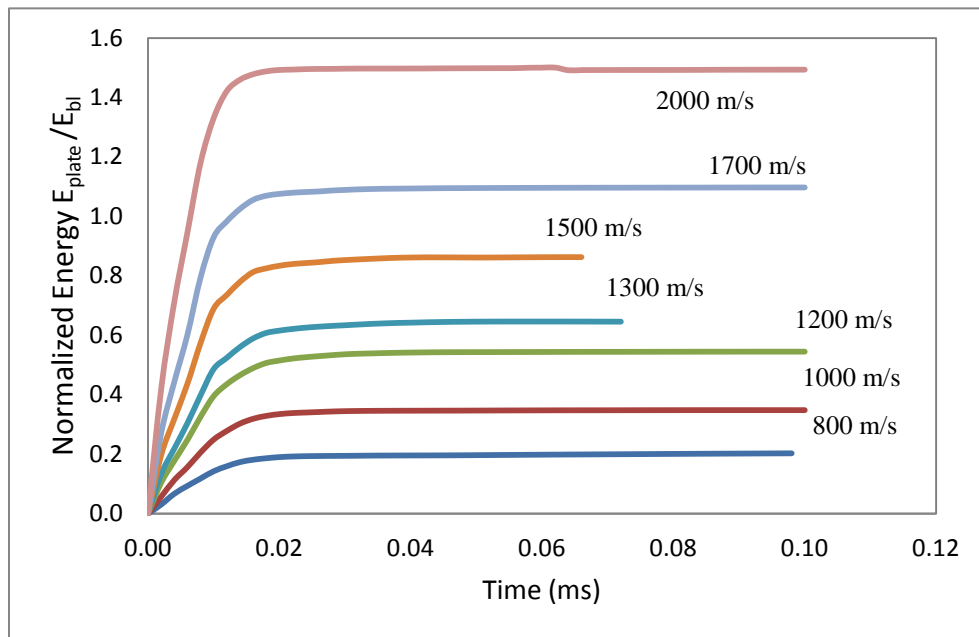


Fig. 9 The energy dissipation of the blank steel plate when impacted by fragment simulating projectile at different impact velocity

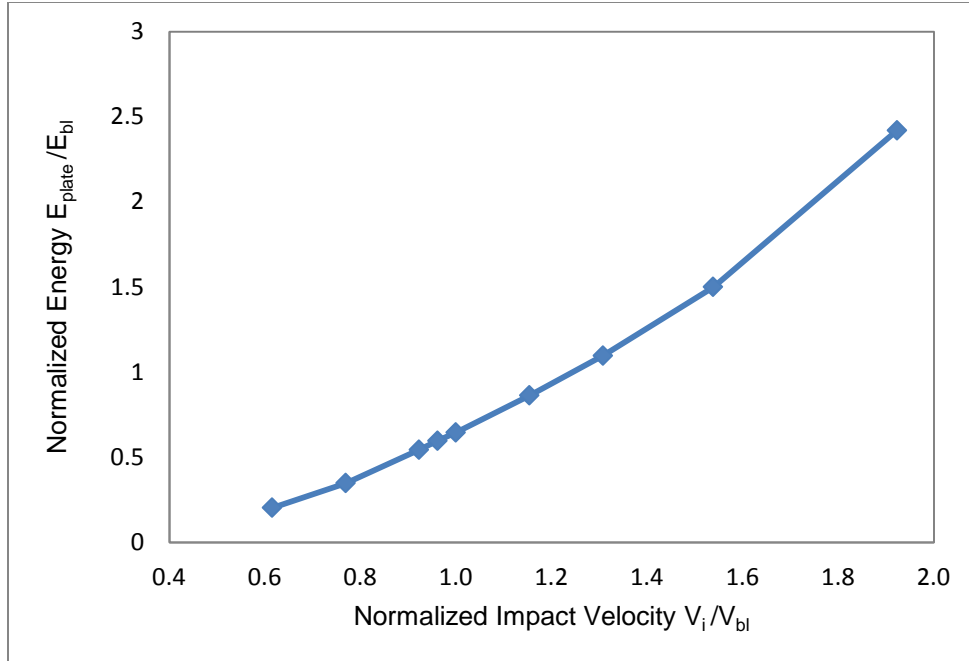
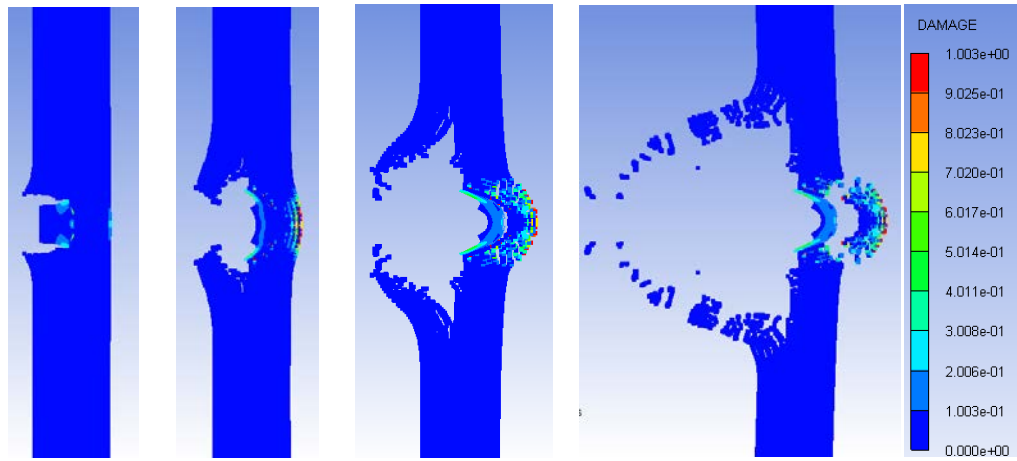


Fig. 10 The energy dissipation of the steel plate vs. the impact velocity of the fragment simulating projectile

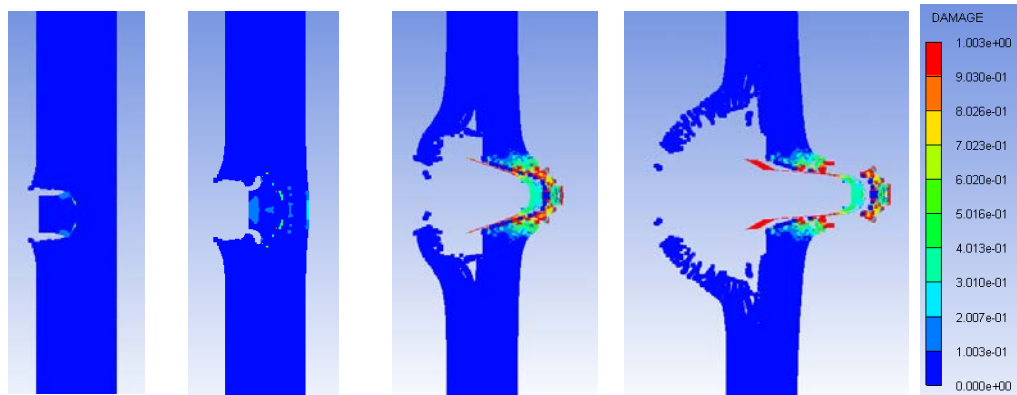
4.3 Ballistic performance of polyurea coated HHS plates

A series of simulations of fragment simulating projectiles striking the same HHS steel plates, but coated with polyurea on the front face, was run with impact velocities ranging from 800 to 2500 m/s. Temporal evolution of the material deformation/damage status within the two layers of the target plates is shown in Fig. 11. It should be noted that the same fracture patterns observed in the blanked steel plate; dishing mode at low impact velocity, shear plug at intermediate velocities, full penetration at higher velocities, and complete fragmentation of penetrated area were also observed here.

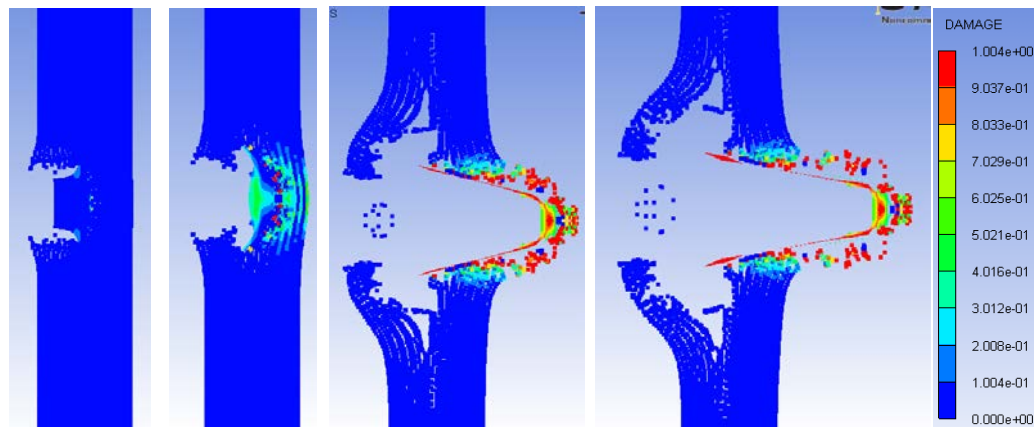
It is clear in Fig. 12 that at the early stage of impact, the pressure field in the target plate is dominated by a shock wave emanating radially from the point of impact. The mechanical response of the target plate and of the projectile is controlled by the polyurea face layer. At the intermediate stages of the impact, when the shock wave reaches the polyurea/steel interface, a negative-pressure region begins to develop at the back face of the polyurea layer. This gives rise to the onset of tensile failure of polyurea in this region. At the later stages of the impact when the projectile has already entered the steel backing layer, a substantially larger region of polyurea has been subjected to negative pressures and, consequently, has failed structurally. Meanwhile, high pressures are observed in the steel layer surrounding the tip of the projectile.



(a) $v_i = 1500$ m/s time = 0.012ms; $t = 0.024$ ms ; $t = 0.054$ ms ; $t = 0.138$ ms

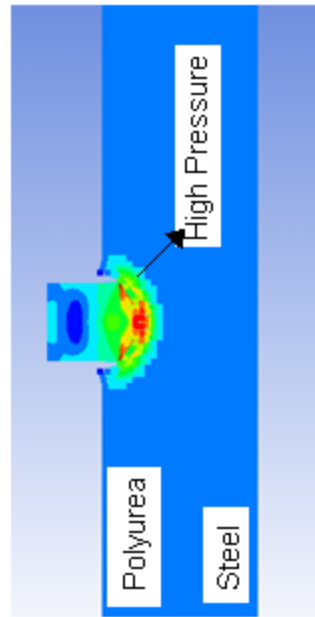


(a) $v_i = 2000$ m/s time = 0.008ms; $t = 0.012$ ms ; $t = 0.038$ ms ; $t = 0.072$ ms

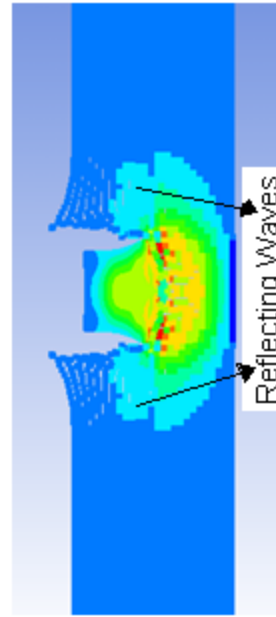


(a) $v_i = 2500$ m/s time = 0.008ms; $t = 0.012$ ms ; $t = 0.038$ ms ; $t = 0.05$ ms

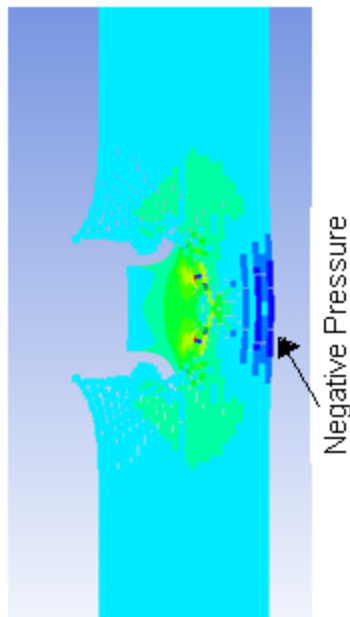
Fig. 11 Deformation and damage status vary at different impact velocities for polyurea coated HHS plate impacted by fragment simulating projectiles.



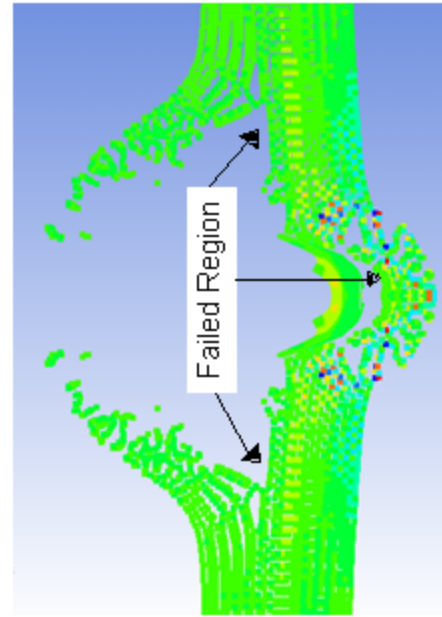
(a)



(b)



(c)



(d)

Fig. 12 Temporal evolution of the pressure within the two layers of the target plates

The residual velocities of the fragment simulating projectile impacting on the polyurea coated steel plate are plotted in Figs. 13 and 14 as a function of the impact velocity.

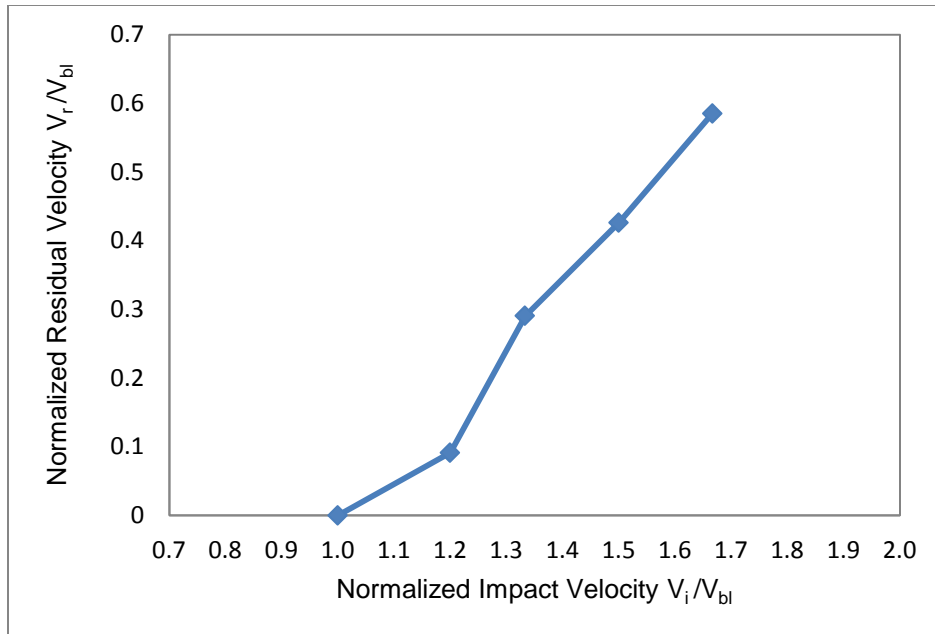


Fig. 13 The residual velocities vs. the impact velocities of the projectile when impacting on polyurea coated steel plate

The x-axis intercept in Fig. 14 represents the approximate V_{50} of the target plates. It was clear that coating the front side of the HHS plate with polyurea leads to an increase the ballistic limit of it.

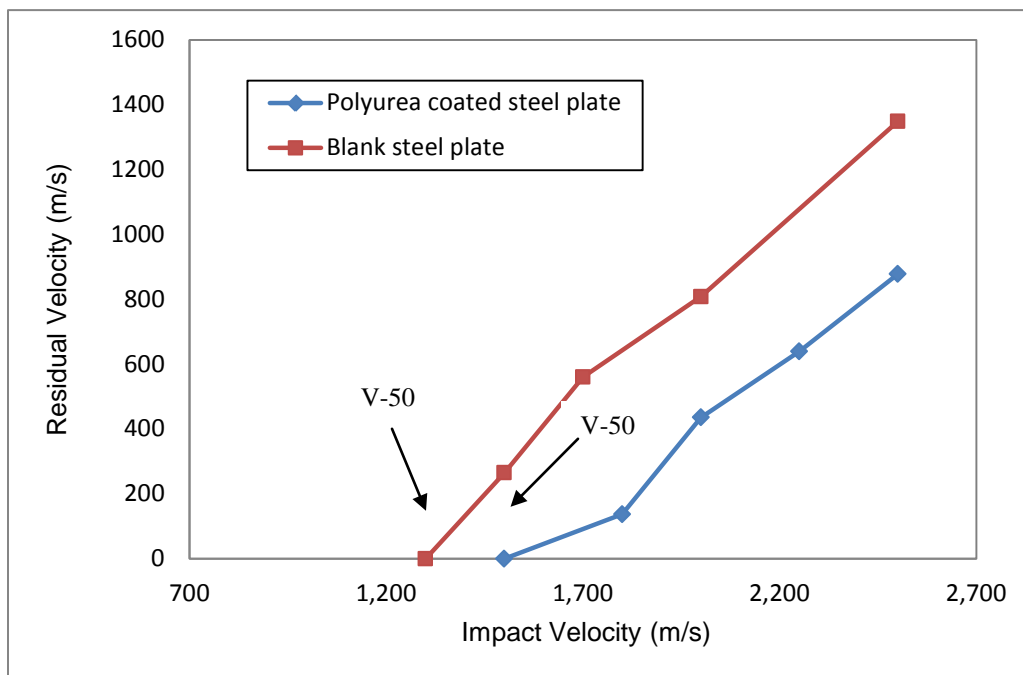


Fig. 14 The residual velocities vs. the impact velocities of the projectile

The energy absorption of the polyurea coated steel plate at the range of the impact velocities by fragment simulation projectile is plotted in Fig. 15. The energy dissipated by the target plate (E_{plate}) is normalized by the initial kinetic energy of the projectile at the ballistic limit $E_{bl} = 1/2 m_{proj} v_{bl}^2$.

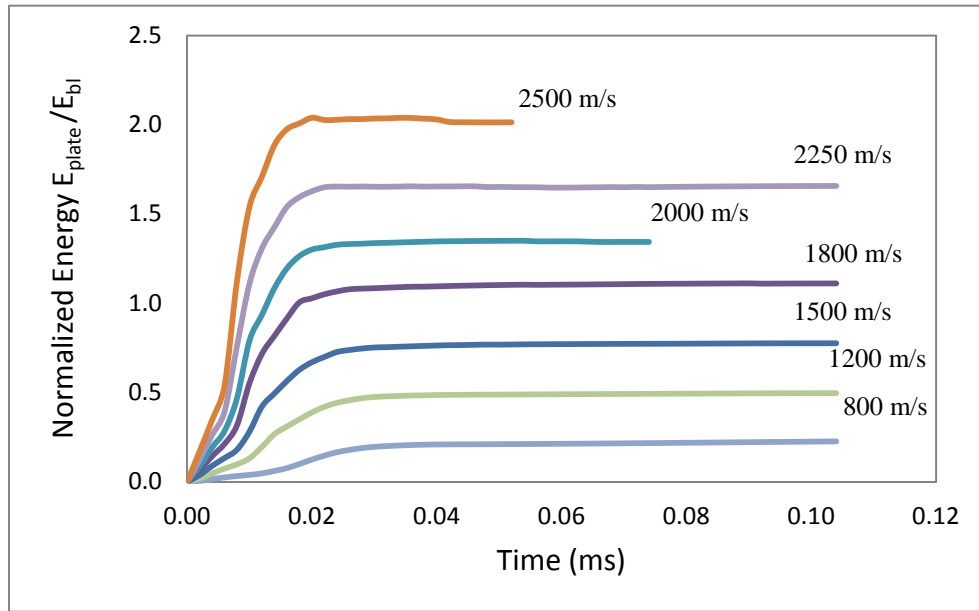


Fig. 15 The energy dissipation of the polyurea coated steel plate when impacted by fragment simulating projectile at different impact velocity

The energy dissipation of the steel plate and the polyurea coating during the impact event for the 1500 m/s impact is in Fig. 16.

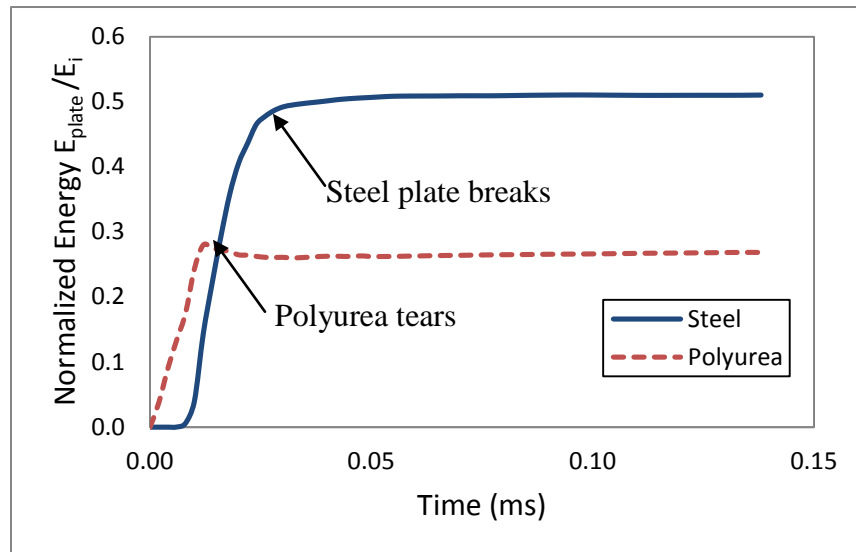


Fig. 16 The energy dissipation portioning of the projectile impacting on a polyurea coated steel plate at 1500 m/s

The energy absorption of the polyurea coated steel plate at the range of the impact velocities by fragment simulation projectile is plotted in Fig. 17. For comparison purposes, the energy absorbed by the blank steel plate is also plotted. It appears that the polyurea serves as a protective layer to delay the fracturing of the steel plate. It was also clear that the energy absorbed by the steel plate increases when coated with polyurea. This increase is denoted by the shaded area in Fig. 17.

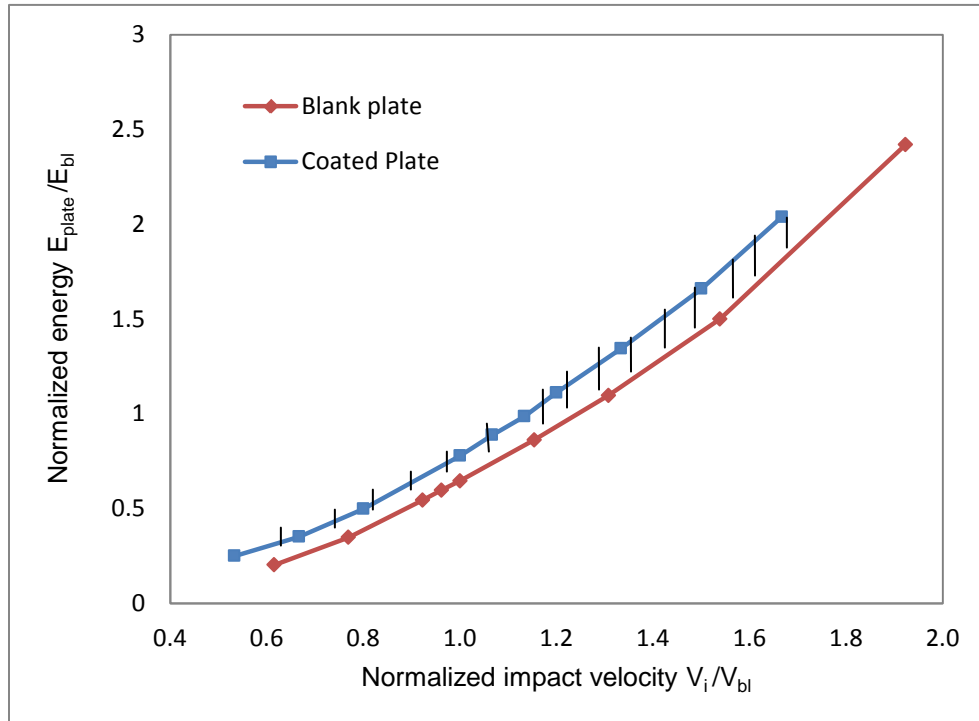


Fig. 17 The energy dissipation of the blank and the polyurea coated steel plates vs. normalized impact velocity of the projectile

4.4 Influence of polyurea coating thickness

The effect of the polyurea coating thickness on the V_{50} is depicted in Fig. 18 and Table 3. An increase in the coating thickness produces a corresponding increase in V_{50} . The results indicate a reduction in slope at higher thickness. Coating thickness represents the distance the projectile has to travel within the target. Large travel distances present a correspondingly large surface for energy dissipation, thus increasing the ballistic limit of the material.

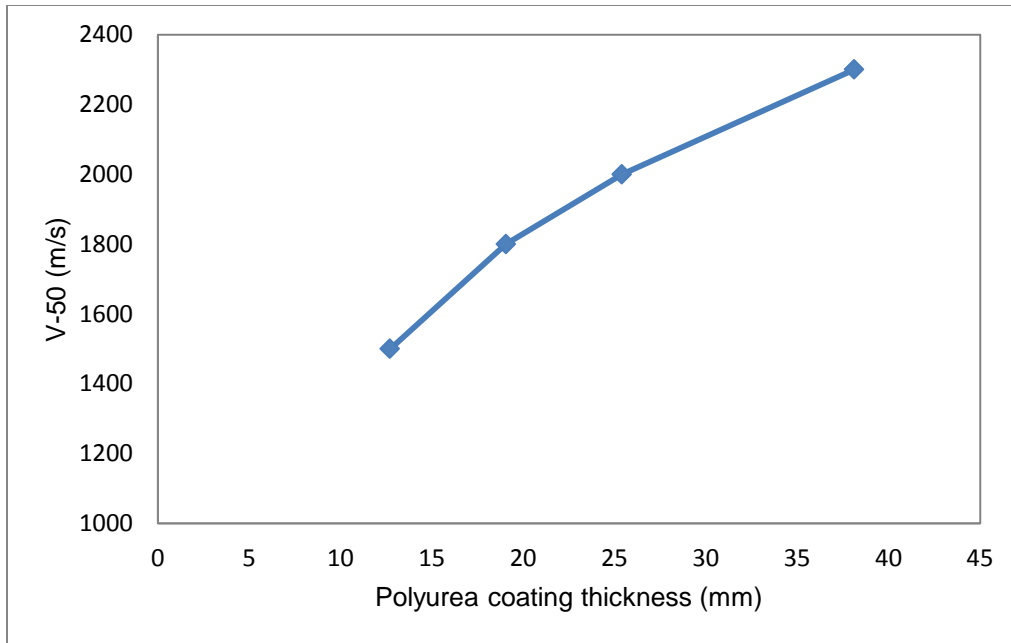


Fig. 18 Effect of polyurea coating thickness on V_{50}

Table 3 Effect of polyurea coating thickness on V_{50}

Polyurea thickness	V-50
6.4	1400
12.7	1500
19.05	1800
25.4	2000

5 Conclusion

In the present work, a nonlinear dynamic analysis of the impact and penetration of High Hard Steel (HHS) plates with and without polyurea coatings is carried out in order to predict their response to ballistic impact by fragment simulating projectiles. A series of hydrocode simulations was performed using AUTODYN in order to predict the ballistic limit (V_{50}) of the target plates. Both Lagrange and SPH techniques are employed. Comparing the computational results with those from the experiments shows that simulations using the SPH technique have the ability to predict the V_{50} of the blank HHS plates and the polyurea coated HHS plates more accurately than Lagrange technique.

The response of the blank HHS plate to the fragment simulating projectile can be divided into four categories. (a) At impact velocities below V_{50} , dishing mode was observed. The kinetic energy of the projectile is dissipated by the plastic deformation of the plate. (b) At impact velocities just a little bit above V_{50} , a shear plug is broken off the steel plate right underneath the impacted area of the projectile. However, the projectile was stopped. (c) At higher velocities, the projectile makes its way through the entire thickness of the steel plate. (d) At even higher impact

velocities, complete fragmentation of the penetrated area into small pieces was observed.

The same fracture patterns observed in the blanked steel plate were also observed in the polyurea coated HHS plate. However, it was clear that coating the front side of the HHS plate with polyurea leads to an increase in the ballistic limit. It was also noted that the polyurea serves as a protective layer to delay the fracturing of the steel plate. It was also clear that the energy absorbed by the steel plate increases when coated with polyurea.

Acknowledgement

This work was partially supported by the funding received under a subcontract from the Department of Homeland Security-Sponsored Southeast Region Research Initiative (SERRI) at the Department of Energy's Oak Ridge National Laboratory, USA. The authors would like to thank Raymond Gamache from Naval Surface Warfare Center and William Laska from Science and Technology Directorate of Department of Homeland Security for their helpful discussions during this study.

References

1. Roland CM, Twigg JN, Vu Y, Mott PH (2007) High strain rate mechanical behavior of polyurea. *Polymer* 48: 574-578.
2. Corbett GG, Reid SR, and Johnson W (1996) Impact loading of plates and shells by free flying projectiles: a review. *Int. J Impact Eng.* 18:141–230.
3. Backman ME, Goldsmith W (1978) The mechanics of penetration of projectiles into targets. *Int. J Eng Sci.* 16:1–99.
4. Xue Z, Hutchinson JW (2008) Neck development in metal/elastomer bilayers under dynamic stretchings. *Int. J Solids Struct* 45:3769–78.
5. Xue Z, Hutchinson JW (2007) Neck retardation and enhanced energy absorption in metal–elastomer bilayers. *Mech Mater* 39:473–87.
6. Malvar LJ, Crawford JE, Morrill KB (2007) Use of composites to resist blast. *J Compos Construct* 11(6):601–10.
7. Amirkhizi AV, Isaacs J, McGee J, Nemat-Nasser S (2006) An experimentally-based viscoelastic constitutive model for polyurea, including pressure and temperature effects. *Philosophical Magazine* 86: 5847-5866.
8. El Sayed T (2007) Constitutive models for polymers and soft biological tissues, Ph.D. Dissertation, California Institute of Technology.
9. El Sayed T, Mock Jr W, Mota A, Fraternali F, Ortiz M (2009) Computational assessment of ballistic impact on a high strength structural steel/polyurea composite plate. *Computational Mechanics* 43:525-534.
10. Li C, Lua J (2009) A hyper-viscoelastic constitutive model for polyurea. *Material Letter* 63:877-880.
11. Roland CM, Fragiadakis D, Gamache RM (2010) Elastomer steel laminated armor. *Composite structures* 92:1059–1064.
12. Bogoslovov RB, Roland CM, Gamache RM (2007) Impact-induced glass transition in elastomeric coating. *Applied Physics Letters* (90) 221910.

13. Grujicic M, Pandurangana B, Hea T, Cheesemanb BA, Yenb CF, Randowb CL (2010) Computational investigation of impact energy absorption capability of polyurea coatings via deformation-induced glass transition. *Material Science and Engineering A* 527:7741-7751.
14. Xue L, Mock Jr. W, Belytschko T (2010) Penetration of DH-36 steel plates with and without polyurea coating. *Mechanics of materials* 42: 981-1003.
15. Amini MR, Isaacs JB, Nemat-Nasser S (2006) Effect of polyurea on the dynamic response of steel plates. *Proceedings of the 2006 SEM Annual Conference and Exposition on Experimental and Applied Mechanics*, St. Louis, MO, June 4-7, 2006.
16. AUTODYN[®] Explicit Software for Nonlinear Dynamic (2005) Theory Manual Revision 4.3, Century Dynamics.
17. Johnson GR, Cook WH (1983) A constitutive model and data for metals subjected to large strains, high strain rates and high temperatures. *Proc 7th Int. Symposium on Ballistics*, Hague, Netherlands, 541–547.
18. Zukas JA (2004) *Introduction to Hydrocodes*. Elsevier, Amsterdam.